STEROL CHEMICAL STRUCTURE AND CONFORMATION INFLUENCE THE THERMOTROPIC PHASE BEHAVIOUR OF DIPALMITOYLPHOSPHATIDYLCHOLINE BILAYERS

Matthew G. K. Benesch, David A. Mannock, & Ronald N. McElhaney
Department of Biochemistry, School of Molecular and Systems Medicine, Faculty of Medicine and Dentistry, University of Alberta

Abstract

Studying the nature of interactions between the sterol ring system and neigbouring phospholipid molecules is important for our understanding of the properties of sterols in biological molecules and the role of such interactions in many disease processes. In this project, the thermotropic phase behaviour of binary dipalmitoylphosphatidylcholine (DPPC)/sterol mixtures with different sterol ring configurations (C5,6 double bond, 5α-H and 5β-H orientation and either 3α-OH, 3β-OH, 3-ketone functional groups) was investigated using differential scanning calorimetry (DSC) and was compared to earlier studies of cholesterol/ and epicholesterol/DPPC mixtures. Given the differences in the thermodynamic parameters obtained from these mixtures and their associated changes in bilayer stability and miscibility, it is clear that changing the sterol chemical configuration has a significant effect on bilayer properties. Any sterol molecule whose ring structure deviates from that of cholesterol is unlikely to be fully miscible in mammalian membranes.
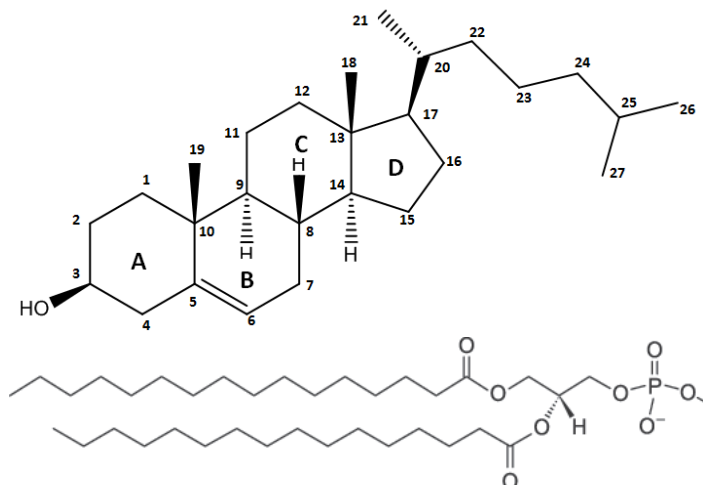
Introduction

The lipid bilayers of biological membranes contain a wide range of phospho- and glycolipids, as well as other amphiphilic molecules differing in their chemical structure. Of those, sterols such as cholesterol (Chol) are among the most commonly identified membrane constituents, modulating the physical properties and lateral organization of the plasma membrane lipid bilayer. Chol has an equatorially orientated C3-OH group in ring A of the steroid nucleus (Fig 1), which has been identified to be planar and rigid, a double bond at C5,6 in ring B, and an alkyl side-chain at C17 of the cyclopentane ring. The small polar headgroup and large hydrophobic ring and side-chain anchor Chol in the phospholipid bilayer with the long axis of the sterol molecule lies parallel to the lipid acyl chains and the polar headgroup sitting in the bilayer interface. Biological membranes are fluid at physiological temperatures but are thought to be regionally heterogeneous, containing lipid microdomains or rafts, which are enriched in tightly-packed, structurally


Figure 1. The chemical structure of a typical sterol (top), cholesterol, with both carbon atom numbering and ring identification. This study investigates the effect of changes in the chemical structure of the steroid ring system on ring conformation and electronics. Changing the stereochemistry at C-3 and removing the carbon 5-6 double bond introduces a new stereocentre at C-5. The chemical structure of 1,2-dipalmitoyl-3-sn-phosphatidylcholine (bottom), the phospholipid matrix used in this study.

important lipids, such as sphingomyelin (SpM) and Chol. These ordered microdomains are surrounded by regions of more disordered lipids, enriched with phosphatidylcholines (PCs) and other phosphoglycerolipids. Lipid rafts from diverse natural sources contain sterols with different chemical configurations, whose structure is supposedly optimized to maintain the permeability, fluidity, elasticity, and curvature of the host membrane. However, relatively little is understood about how systematic changes in sterol structure affect those physical parameters through their interactions with surrounding lipid molecules. Nevertheless, the various sterol structures differ in their effects on the chain-melting phase transition of the host membrane lipids and in their condensing and ordering of the liquid-disordered bilayer to create liquid-ordered domains, which differ in their bulk physical properties relative to a sterol-free bilayer composition.

Several important human and mammalian diseases have been associated with the membrane sterol content and with lipid rafts in particular. These include neurodegenerative diseases such as Parkinson's and Alzheimer's (1-3), viral- (4-6) and prion-associated diseases (7,8), bacterial infections (9), as well as diabetes (10) and some cancers (11,12), all of which have a common site of action on the cell membrane: the lipid rafts (13). In these diseases, metabolic dysfunctions or the binding of infectious agents disrupt the cell biochemistry by means of associated physical mechanisms (11-14), eventually leading to changes in cell metabolism and, through changes in lipid signaling pathways, producing either cell growth or death and disease manifestation (15). Recent studies indicate that once the above processes begin, lipid raft reorganization occurs because of the separation of the lipid constituents and their lateral redistribution (16,17), together with changes in the localized concentration of important proteins and cell surface antigens on the membrane surface (17,18). However, how changes in lipid and sterol structure influence these demixing processes are not completely understood.

Our understanding of the nature of interactions between sterol and lipid molecules in biological membranes is also

incomplete. While there have been many investigations into the effects of Chol on the gel/liquid-crystalline (Pα/Lα) phase transition of model phospholipids with a range of headgroup structures and with either saturated or unsaturated acyl chains (19-26), there have been relatively few studies in which the sterol tetracyclic ring and isooctyl side-chain have been systematically varied. This situation arises because of the limited number of natural sterols that are commercially available at reasonable cost and the absence of a substantial pool of sterol structural motifs among those products. Thus, it is difficult to understand the roles played by variations in the number of functional groups, their position, and orientation in the tetracyclic ring system and the alkyl side-chain and, consequently, the changes in the conformational and electronic contributions arising from each sub-structure. All of these contributions affect the sterol molecular conformation and modify the bilayer physical properties.

Previous work in our laboratory used differential scanning calorimetry (DSC) to study the thermotropic phase behavior of binary Chol and epicholesterol (EChol; axial C3-OH group)/dipalmitoylphosphatidylcholine (DPPC) mixtures (24). Summarized briefly, the Chol/EChol study indicated that the incorporation of EChol is more effective than Chol in reducing the enthalpy of the pretransition of DPPC and is initially more effective than Chol in reducing the enthalpies of both the sharp and broad components of the main phase transition of DPPC, which arising from the sterol-poor and sterol-rich regions, respectively. However, at 30-50 mol% EChol sterol concentrations, EChol becomes less effective than Chol in reducing the enthalpy and cooperativity of the main phase transition, such that although at sterol concentrations of 50 mol%, EChol, unlike Chol, does not completely abolish the cooperative hydrocarbon chain-melting phase transition of DPPC, it does not appear to form a calorimetrically detectable micro-crystalline phase at higher sterol concentrations. This illustrates the importance of Chol in biological membranes. Spectroscopic and other results indicate that monomeric EChol is less miscible in DPPC bilayers than is Chol at higher sterol concentrations, but perturbs their organization to a greater extent at lower concentrations, probably due to the lower position of EChol in the bilayer interface.

This evolving molecular perspective from previous work on binary sterol/DPPC mixtures is extended here to include the cholesterol ketone (5-cholesten-3-one, CholK), and four sterols and two steroids with no double bond in ring B with the 5α-H and 5α-H conformation at the junction of rings A and B and either a 3α-OH, 3α-OH, or 3-ketone functional group. Two- and three-dimensional structures of these sterols and steroids are shown in Figs 2-4. The 5α-H and 5α-H sterols (corprostanol and epicoprostanol, respectively) are found in sewage and marine sediments and soil, and are thought to be Chol reduction products produced by gut and soil bacteria (27). The steroids are oxidation products of the corresponding alcohols and are early intermediates in the biosynthesis of bile acids and hormones (28).
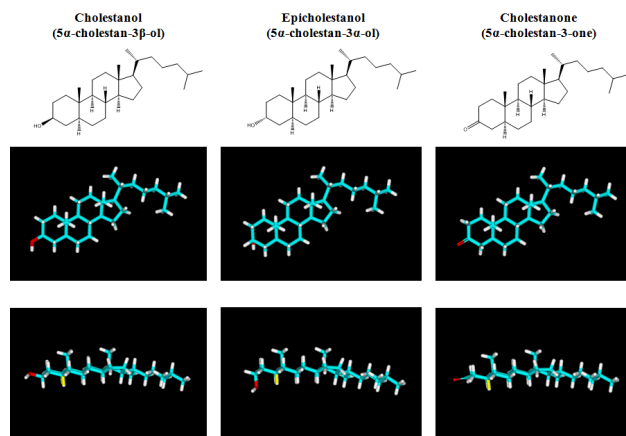
Figure 2. Molecular models of cholesterol (left column), epicholesterol (middle column), and keto-cholesterol (right column). The top row panels show the 2D structure of these sterols, the middle row panels show views normal to the plane of the sterol ring and the bottom row panels show views parallel to the plane of the sterol ring. The C-3 hydroxyl and ketone groups are colored in red. The molecules were minimized using DSviewer 5.0 (Accelrys Software Inc., San Diego, CA).
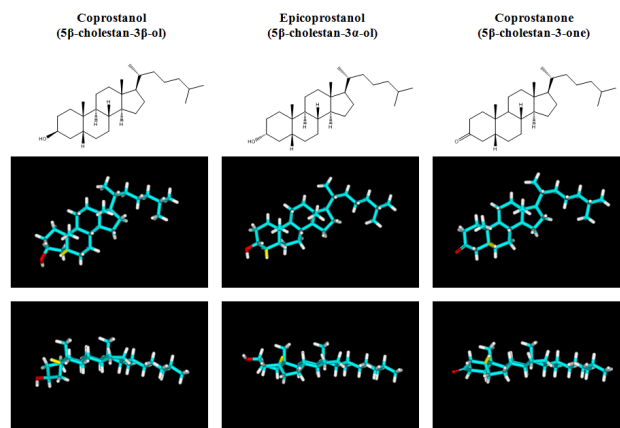
Figure 3. Molecular models of 5α-cholestan-3β-ol (left column), 5α-cholestan-3α-ol (middle column), and 5α-cholestan-3-one (right column). The top row panels show the 2D structure of these sterols, the middle row panels show views normal to the plane of the sterol ring and the bottom row panels show views parallel to the plane of the sterol ring. The C-3 hydroxyl and ketone group are colored in red and the 5α proton is highlighted in yellow. The molecules were minimized using DSviewer 5.0 (Accelrys Software Inc., San Diego, CA).
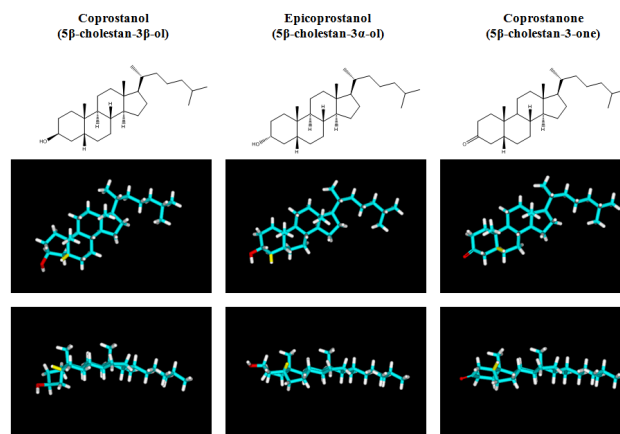
Figure 4. Molecular models of 5β-cholestan-3β-ol (left column), 5β-cholestan-3α-ol (middle column), and 5β-cholestan-3-one (right column). The top row panels show the 2D structure of these sterols, the middle row panels show views normal to the plane of the sterol ring and the bottom row panels show views parallel to the plane of the sterol ring. The C-3 hydroxyl and ketone group are colored in red and the 5α proton is highlighted in yellow. The molecules were minimized using DSviewer 5.0 (Accelrys Software Inc., San Diego, CA).

Experimental Procedures

The DPPC and Chol (both 99% pure) were both obtained from Avanti Polar Lipids (Alabaster, AL), whereas the remaining sterols and steroids (all 98% pure by TLC) were supplied by Steraloids Inc. (Newport, RI). All organic solvents were analytical grade and were redistilled before use. Hydrated samples for DSC were prepared exactly as described previously (23). The dry DPPC:sterol films were dispersed in 1 ml deionized water by vigorous vortex mixing at temperatures near 55-60 °C, degassed, and 900 μl aliquots were used for gathering DSC thermograms of the main phase transition using a high-high sensitivity multi-cell DSC instrument and 324 μl aliquots for the pretransition using a high-sensitivity Nano DSC (both from Calorimetry Sciences Corporation, Lindon, UT), at a scan rate of 10 °C/h. The quantity of lipid in the DSC samples was progressively increased with additional sterol content to ensure better resolution of the broad low-enthalpy thermotropic transitions, as described earlier (25).

The data were analyzed using Origin 7.5 (OriginLab Corporation, Northampton, MA). The midpoint temperatures, peak widths at half height (inversely related to cooperativity) and areas of the components (proportional to the enthalpy) seen in complex endotherms were estimated with the aid of the Origin non-linear least squares curve- and peak-fitting procedures and a custom-coded function based on the assumption that the observed thermogram is a linear combination of components, each of which could be approximated by a reversible two-state transition at thermodynamic equilibrium. The equations used to develop the fitting function are described elsewhere (29).

Results

The overall pattern of thermotropic phase behaviour observed in sterol/DPPC dispersions

DSC heating scans of DPPC dispersions containing different concentrations of the nine sterols and steroids are shown for comparative purposes in Fig 5. In the absence of sterols, DPPC heating scans show two sharp endothermic peaks initially centered ~35 °C and ~41.7 °C, which correspond to the so-called pretransition, a transition from a lamellar gel phase with tilted hydrocarbon chains to a rippled gel phase with tilted hydrocarbon chains (Lα'/Pα'), and a main phase transition from a rippled gel phase to a liquid-crystalline phase (Pα'/Lα), respectively. From these thermograms, we can measure the phase transition temperature, T (°C), as a function of sterol concentration. Increases in T reflect the ability of the sterol to stabilize and order the DPPC gel phase. Corresponding measurements of $\Delta T_{1/2}$ (°C), the width of the phase transition at half height, which is inversely related to the cooperativity of the phase transition, measures the ability of the sterol to broaden the phase transition. Increasing the concentration of molecule A (sterol) in molecule B (lipid) typically increases $\Delta T_{1/2}$ if the two molecules are miscible. The phase transition enthalpy, ΔH (kcal/mol), is a measure of the energy required for the lipid/sterol mixture to undergo a phase change. The ability of the sterol to abolish the phase transition can be positively correlated to the miscibility of the sterol in the DPPC bilayer. If $\Delta H = 0$, the sterol is essentially fully miscible in the bilayer.

Normally in sterol/DPPC mixtures, increasing the sterol concentration gradually reduces the pretransition temperature (T_p), broadens the pretransition ($\Delta T_{p1/2}$), and eventually abolishes the enthalpy (ΔH_p). Similarly, for the main phase transition, increasing the sterol concentration initially produces a multi-component endotherm that consists of a sharp component that is progressively reduced in temperature (T_m^{shp}), broadened ($\Delta T_{1/2}^{shp}$) and reduced in enthalpy (ΔH_m^{shp}), and a broad component that may either increase (increase stability) or decrease (decrease stability) in temperature (T_m^{brd}), broaden ($\Delta T_{1/2}^{brd}$), and normally initially increase, then decrease in enthalpy (ΔH_m^{brd}). Overall, with increasing sterol concentration, the sharp component disappears as the broad component grows, and the sum of these two components gives the total enthalpy of the main phase transition (ΔH_m^{tot}). However, there are important qualitative differences in the effect of sterol ring structure and conformation on the DPPC pretransition and on the two components of the main phase transition, as discussed below.
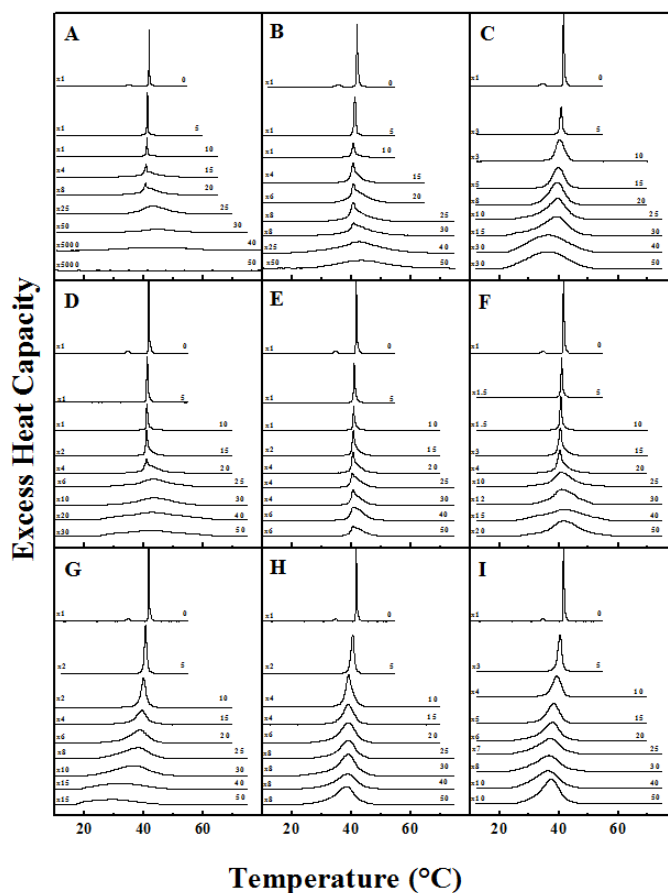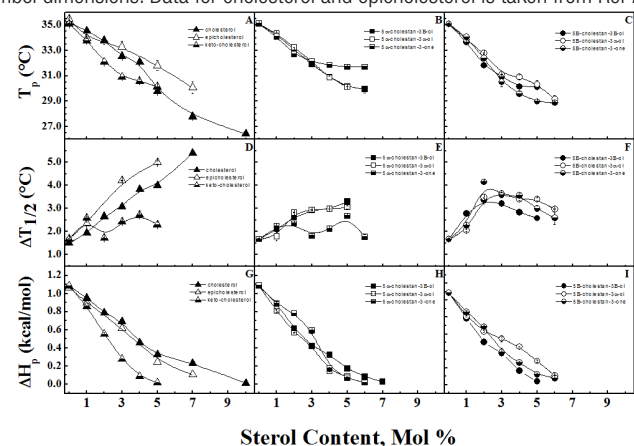

Figure 5. DSC thermograms illustrating the effect of cholesterol1 (A), epicholesterol1 (B), 5-cholesten-3-one (C), 5α-cholestan-3β-ol (D), 5α-cholestan-3α-ol (E), 5α-cholestan-3-one (F), 5β-cholestan-3β-ol (G), 5β-cholestan-3α-ol (H), and 5β-cholestan-3-one (I) on the gel/liquid-crystalline phase transition of DPPC. The mixtures were heated and cooled at 10 °C/h (to maximize resolution and minimize artifacts). The thermograms shown were acquired at the sterol concentrations (mol%) indicated and have all been normalized against the mass of DPPC used. Y-axis scaling factors are indicated on the left-hand side of each thermogram.[1] Ref 24.

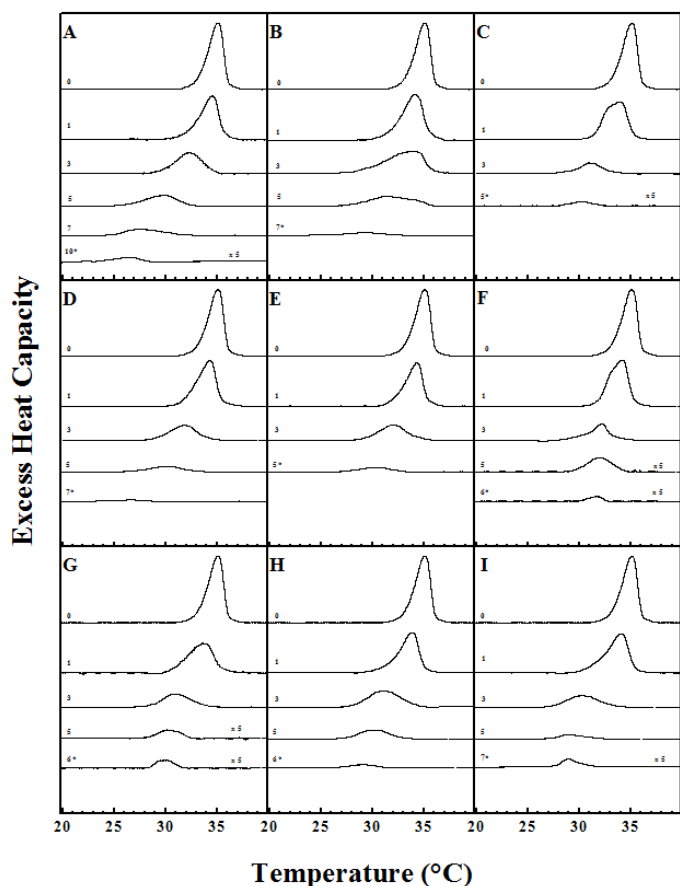*The effects of sterols on the pretransition of DPPC*

The gradual elimination of the pretransition in the DSC heating scans with increasing sterol concentration are shown in Fig 6 and the derived thermodynamic parameters defined above are shown in Figs 7 (grouped by the functional group at carbon 3) and 8 (grouped by the conformation of carbon 5). All sterol/DPPC mixtures show a reduction in T_p with increasing sterol concentration (Figs 7,8 A-C), but mixtures containing the steroids are more effective at destabilizing the Lα' phase and at perturbing the phase transition than the corresponding sterols. A notable exception to this trend is 5α-H,3-K, where T_p levels off at ~32 °C. The 3α-ols destabilize the Lα' phase less than 3α-ols, with the largest differences of ~2 °C within the C5,6 double bond group (3α-ol, 3α-ol, 3-K), but shows almost perfect overlap within the 5α-H group (3α-ol, 3α-ol, 3-K). $\Delta T_{p½}$ increases most rapidly for EChol and Chol, demonstrating their ability to better disorder the pretransition (Figs 7D, 7E, 8D). The 5α-H sterols have a similar effect on the DPPC transition, although the 5α-H,3α-ol/5α-H,3α-ol pair show fewer differences between each other than those of the EChol/Chol pair (Figs 8D & E). When the data from the three ketones are compared (5α-H, 5β-H, C5,6 double bond), the curves reach a maximum at
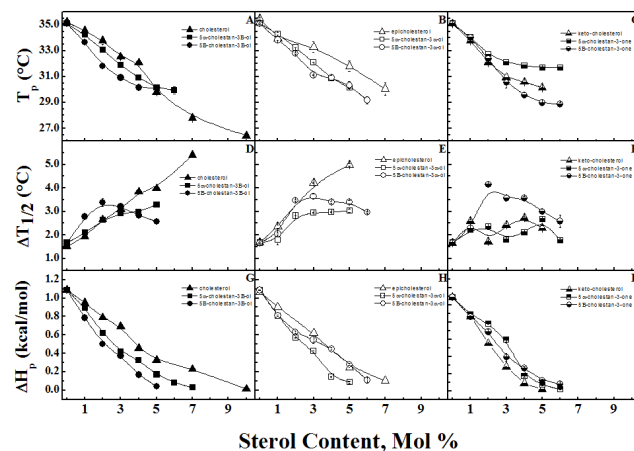
Figure 7. The effect of increases in sterol concentration on Tp (A-C), △T1/2 (D-F), and △Hp (G-I) on the pretransition of DPPC. These parameters are grouped by C-3 functional group. The left column is the C-3β-hydroxyl sterols, the middle column is the C-3α-hydroxyl sterols, and the right column is the C-3-keto-steroids. When a standard error bar is not visible, it is less than or equal to the symbol dimensions. Data for cholesterol and epicholesterol is taken from Ref 24.

Figure 8. The effect of increasing sterol concentration on Tp (A-C), △T1/2 (D-F), and △Hp (G-I) on the pretransition of DPPC. These parameters are grouped by C-5 functional group. The left column is C-5,6-double-bond sterols, the middle column is 5α-sterols, and the right column is 5β-sterols. When a standard error bar is not visible, it is less than or equal to the symbol dimensions. Data for cholesterol and epicholesterol is taken from Ref 24.

Figure 6. DSC thermograms illustrating the effect of cholesterol1 (A), epicholesterol1 (B), 5-cholesten-3-one (C), 5α-cholestan-3β-ol (D), 5α-cholestan-3α-ol (E), 5α-cholestan-3-one (F), 5β-cholestan-3β-ol (G), 5β-cholestan-3α-ol (H), and 5β-cholestan-3-one (I) on the pre-transition of DPPC. The mixtures were heated and cooled at 10 °C/h (to maximize resolution and minimize artifacts). The thermograms shown were acquired at the sterol concentrations (mol%) indicated on the panels left side and have all been normalized against the mass of DDPC used. Y-axis scaling factors are indicated on the right-hand side of each thermogram. The * indicate the highest mol% where the pre-transition was observed.[1] Ref24.
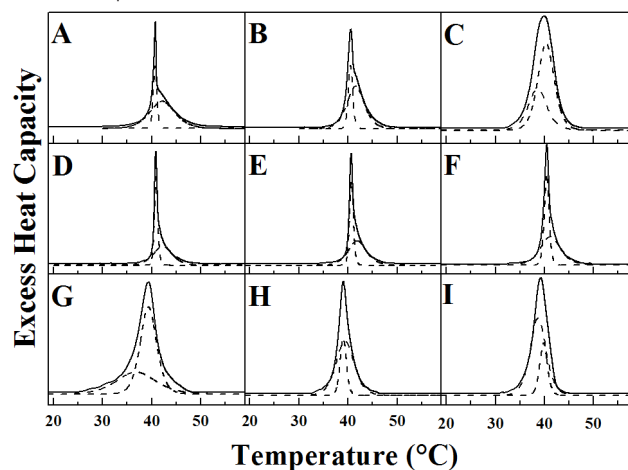
Figure 9. Typical peak-fitting deconvolution analysis of the DSC thermograms exhibited by 15 mol% cholesterol1 (A), 15 mol% epicholesterol1 (B), 15 mol% 5-cholesten-3-one (C), 15 mol% 5α-cholestan-3β-ol (D), 15 mol% 5α-cholestan-3α-ol (E), 15 mol% 5α-cholestan-3-one (F), 15 mol% 5β-cholestan-3β-ol (G), 10 mol% 5β-cholestan-3α-ol (H), and 10 mol% 5β-cholestan-3-one/DPPC (I) mixtures heated and cooled at 10°C/h . To facilitate visibility, the filled curves are slightly displaced along the y-axis. The analysis is performed using a custom coded algorithm for a first-order phase transition.[1] Ref 24.

~3 mol% and then decrease (Fig 7F). Similar behaviour is observed in a comparison of the $\Delta T_{p\frac{1}{2}}$ values for 5α-H (3α-ol, 3α-ol, 3-K), but the result is less consistent and shows more scatter (Fig 8E). In the case of 5α-H (3α-ol, 3α-ol, 3-K), the curves smoothly and consistently achieve a maximum $\Delta T_{p\frac{1}{2}}$ of ~3-4 °C before steadily decreasing to ~2 °C (Fig 8F), suggesting the existence of at least two components in their pretransition endotherms. The significance of this observation is discussed later.

All sterols and steroids are more effective in decreasing ΔH_p than Chol (Fig 7,8 G-I), abolishing the pretransition by ~5-7 mol%, whereas it persists up to ~10 mol% in the Chol/DPPC mixtures. This indicates that these sterols and steroids occupy a larger cross-sectional area than Chol and/or disorder the hydrocarbon chains of adjacent DPPC molecules to a greater extent. This allows relief of the area mismatch between the relatively larger PC polar headgroups and the relatively smaller hydrocarbon chains, such that energetically unfavorable chain tilting is not required at lower sterol concentrations. Among all of the 3α-ols (5α-H, 5α-H, C5,6 double bond), the 5α-H sterol more effectively abolishes the pretransition than the 5α-H sterol (5 mol% versus 7 mol%; Fig 7G), In contrast, with the 3α-ols (5α-H, 5α-H, C5,6 double bond), the 5α-H sterol more effectively abolishes the pretransition than the 5α-H sterol (Fig 7H). The trends change for the steroids, with CholK more effectively abolishing the pretransition, and 5α-H,3-K being the least effective below 4 mol%, and 5α-H,3-K being the most effective at higher concentration (Fig 7I). A comparison based on the C5,6-conformation shows that within this group, CholK more effectively abolishes the pretransition than either Chol or EChol, with EChol being marginally better at reducing the enthalpy than Chol (Fig 8G). The plots show more overlap for the 5α-H and 5α-H groups, with 5α-H,3-K being the least disruptive below 3 mol%, but 5α-H,3α-ol and 5α-H,3-K appear to be equally more disruptive than 5α-H,3α-ol at higher sterol concentrations (Fig 8H). For the 5α-H group, the 3α-ol most effective abolishes the pretransition, whereas like 5α-H,3-K, 5β-H,3-K is initially the least disruptive, but becomes more effective than the 5α-H,3α-ol above 2 mol% (Fig 8I).

The effects of sterol concentration on the main phase transition of DPPC

The DSC data shown in Fig 5 indicates that at low to moderate sterol concentrations, all sterol-containing DPPC bilayers exhibit asymmetric thermograms for the main P_b'/L_a phase transition, which consists of overlapping sharp and broad thermal events representing the melting of sterol-poor and sterol-rich domains respectively (Fig 9). For the deconvolved sterol-poor component of DPPC/Chol mixtures, T_m^{shp} decreases (destabilization of the Pα' phase), $\Delta T_{\frac{1}{2}}^{shp}$ increases (perturbation of the phase transition of the sterol-poor domain), and ΔH_m^{shp} decreases (abolishing the sterol-poor domain phase transition). The broad component shows a more complex dependence on sterol content and, in most cases, is the only component persisting at higher sterol concentrations. Perhaps the most significant observations are that for DPPC/Chol mixtures: T_m^{brd} continues to increase at high sterol concentrations,
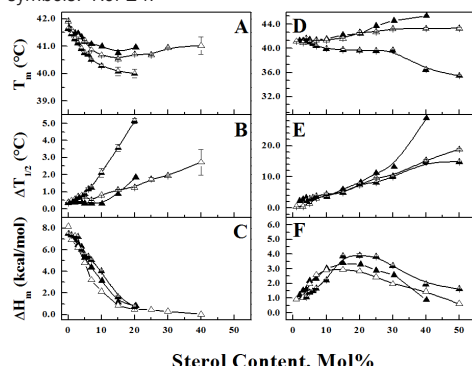
signifying a stabilization of the gel state. Concurrently, the $\Delta T_{\frac{1}{2}}^{brd}$ increases significantly above 30 mol% sterol and the ΔH_m^{brd} is completely abolished, indicating that additional Chol enters the DPPC bilayer and that it is fully miscible with DPPC at higher concentrations. This forms a stable and ordered lamellar phase. However, there are significant differences in the trends observed in the thermodynamic parameters obtained from binary lipid/sterol mixtures with changes in sterol structure (23-25) indicating the subtle influences of sterol structure on the DPPC gel and liquid-crystalline bilayer properties, which have been largely ignored in favor of the myth that Chol possess a rigid ring system with a flexible but fully extended side chain. In the sections below, a detailed report is provided about the effects of changes in sterol ring chemical structure on the sharp and broad components of the DPPC main phase transition and their potential consequences on lateral phase separation in lipid rafts.

The effects of sterols on the sharp component of the DPPC main phase transition

Panels A of Figs 10-12 shows a gradual decrease in T_m^{shp} with increasing sterol concentrations for each sterol/DPPC system. Among the 3β-ols, 5β-H,3β-ol shows the greatest decrease in T_m^{shp} and, thus, the greatest gel phase destabilization. In contrast, 5α-H,3β-ol and Chol show similar curves in which there is only moderate destabilization (Fig 10A). Whereas The $\Delta T_{\frac{1}{2}}^{shp}$ of 5β-H,3β-ol broadens rapidly up to 15 mol%, those of Chol and 5α-H,3β-ol increase more slowly and persist up to 20 mol% sterol (Fig 10B). On the other hand, there is not much difference in the ΔH_m^{shp} values for the 3β-ols, where the transition is abolished between 15 mol% for the 5β-H,3β-ol and 20 mol% for both Chol and 5α-H,3β-OH (Fig 10C). This suggests that C5-conformation changes do not significantly alter the ability of the 3β-ols to abolish the transition in the sterol-poor domains. Among all of the 3α-ols, 5β-H,3α-ol shows the greatest decrease in T_m^{shp}, but the sharp component of EChol and 5α-H,3β-ol level off at 10-15 mol% sterol and persist until 40 mol% and 50 mol% sterol, respectively. This may indicate a difference in the sterol concentration-dependent partitioning between the sterol-poor and sterol-rich domains (Fig 11A). Corresponding $\Delta T_{\frac{1}{2}}^{shp}$ values show that 5β-H,3α-ol has the greatest ability to broaden the main transition sharp component at low sterol concentrations, while EChol and 5α-H,3α-ol are more effective at higher sterol concentrations (Fig 11B). Up to ~7 mol%, all three 3α-ols (5α-H, 5α-H, C5,6 double bond) show the same negative enthalpy coefficients. EChol though does not abolish the sharp component by 40 mol% and 5α-H,3α-ol is the least effective overall, showing a value of ~1 kcal/mol at 50 mol% sterol (Fig 11C). The steroids (5α-H, 5α-H, C5,6 double bond) are similar in the initial decrease of $\Delta T_{\frac{1}{2}}^{shp}$, indicating that they destabilize the $P_{b'}$ phase to the same extent (Fig 12A). 5β-H,3-K is marginally better at broadening the main transition below 7 mol% steroid than CholK. Above 7 mol% steroid, CholK significantly broadens the gel/liquid crystalline phase transition of the sterol-poor region, whereas 5α-H,3-K is only moderately effective. (Fig 12B). The steroids abolish the sharp component of the
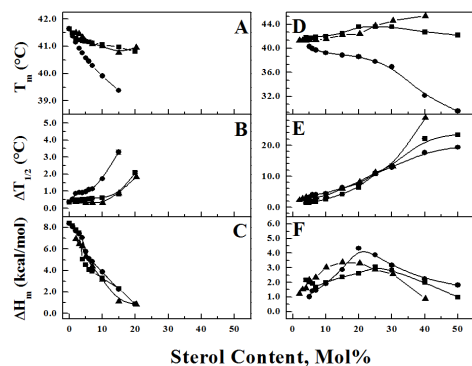
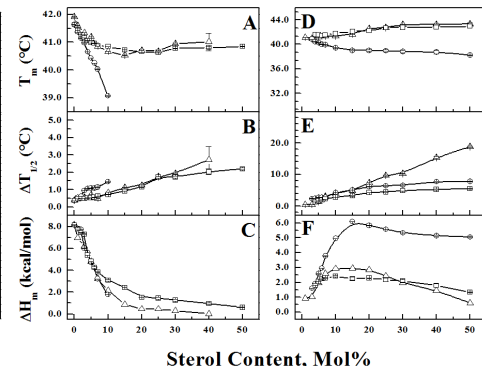**Figure 10.** The thermodynamic parameters of 3β-OH sterols for the deconvolved sharp (A-C) and broad (D-F) components obtained from DSC heating thermograms of cholesterol[1] (▲), 5α-cholestan-3β-ol(■), and 5β-cholestan-3β-ol (●)/DPPC mixtures as a function of sterol concentration. The error bars were typically equal to or smaller than the size of the symbols.[1] Ref 24.

Figure 11. The thermodynamic parameters of 3α-OH sterols for the deconvolved sharp (A-C) and broad (D-F) components obtained from DSC heating thermograms of epicholesterol[1] (△), 5α-cholestan-3α-ol (□), and 5β-cholestan-3α-ol (○)/DPPC mixtures as a function of sterol concentration. The error bars were typically equal to or smaller than the size of the symbols. 1. Ref 24.

Figure 12. The thermodynamic parameters of C-3-keto-sterol for the deconvolved sharp (A-C) and broad (D-F) components obtained from DSC heating thermograms of 5-cholesten-3-one (▲),5α-cholestan-3-one (■), and 5β-cholestan-3-one (●)/DPPC mixtures as a function of sterol concentration. The error bars were typically equal to or smaller than the size of the symbols.
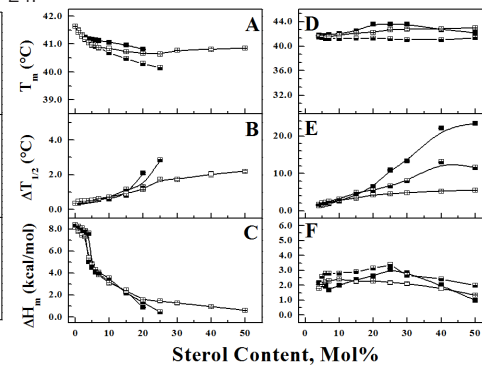
Figure 13. The thermodynamic parameters of C-5,6 double-bond sterols for the deconvolved sharp (A-C) and broad (D-F) components obtained from DSC heating thermograms of cholesterol1 (▲), epicholesterol1 (△), and keto-cholesterol (▲)/DPPC mixtures as a function of sterol concentration. The error bars were typically equal to or smaller than the size of the symbols.[1] Ref 24.

Figure 14. The thermodynamic parameters of 5α-H sterols for the deconvolved sharp (A-C) and broad (D-F) components obtained from DSC heating thermograms of 5α-cholestan-3β-ol (■), 5α-cholestan-3α-ol (▯), and 5α-cholestan-3-one (▤)/DPPC mixtures as a function of sterol concentration. The error bars were typically equal to or smaller than the size of the symbols.

Figure 15. The thermodynamic parameters of 5β-H sterols for the deconvolved sharp (A-C) and broad (D-F) components obtained from DSC heating thermograms of 5β-cholestan-3β-ol (●), 5β-cholestan-3α-ol (○), and 5β-cholestan-3-one (◓)/DPPC mixtures as a function of sterol concentration. The error bars were typically equal to or smaller than the size of the symbols.

main transition fairly similarly with 5β-H,3-K being the best, disappearing at 10 mol%, whereas 5α-H,3-K persists to 25 mol% (Fig 12C).

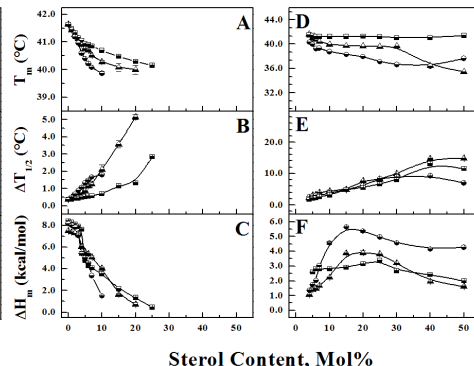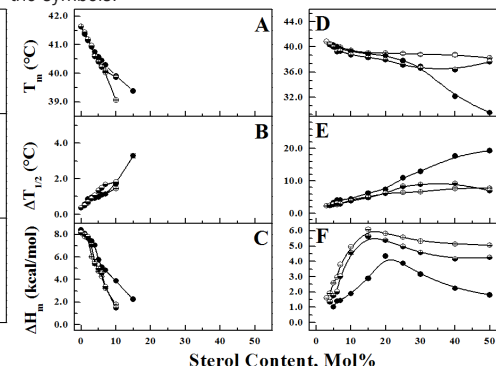Figs 13-15 re-plot the data from Figs 10-12 by C5-conformation. Generally speaking, for the sharp component, steroids (5α-H, 5α-H, C5,6 double bond) are the best able to destabilize the $P_{b'}$ phase and the 3β-ols (5α-H, 5α-H, C5,6 double bond) show the least ability (Figs 13-15 A). The C5,6 double bond group (3α-ol, 3α-ol, 3-K) shows the greatest spread of T_m^{shp} curves, but the 5β-H group (3α-ol, 3α-ol, 3-K) has the greatest overlap over the entire range of concentrations (Fig 13A, 15A). There is variance among the $\Delta T_{1/2}^{shp}$ curves based on the grouping by C5-conformation, but overall, the steroids (5α-H, 5α-H, C5,6 double bond) broaden the main transition more quickly at low concentrations than the sterols (5α-H, 5α-H, C5,6 double bond) (Fig 13-15 B). Unlike the 5α-H sterols (3α-ol, 3α-ol) and C5,6 double bond sterols (3α-ol, 3α-ol), the 5β-H sterols (3α-ol, 3α-ol) abolish the sharp component completely by 10-15 mol% (Fig 15C), whereas 5α-H,3α-ol and EChol do not readily abolish the sharp transition (Fig 13C, 14C). This suggests that sterol concentration-dependent partitioning between sterol-poor and sterol-rich domains is more definitive for the 5β-H sterols (3α-ol, 3α-ol) on account of the 5β-H distorted conformation.

The effects of sterols on the broad component of the DPPC main phase transition

Among all the sterols, Chol is the most effective at stabilizing the Pα' phase in the sterol-rich gel state showing a net temperature shift of ~+2.5 °C by 40 mol%. However, 5β-H,3β-ol is the most destabilizing, displaying a -12 °C shift at 50 mol% sterol. The 5α-H,3β-ol shows intermediate behaviour, increasing to ~+2 °C by 20 mol% before coming back to ~0 °C net temperature shift at 50 mol% concentration (Fig 10D). Whereas the 5β-H,3β-ol is the least able to broaden the main transition among the 3β-ols, the $\Delta T_{1/2}^{brd}$ rapidly increases for Chol at 30-40 mol% sterol (Fig 10E). For the ΔH_m^{brd} curves, peak maxima occur at about 15% for Chol, 20% for 5β-H,3β-ol, and 25% for 5α-H,3β-ol. 5β-H,3β-ol is the least able to abolish ΔH_m^{brd}, whereas Chol is the most effective (Fig 10F).

Similar trends are observed for the 3α-ols (5α-H, 5α-H, C5,6 double bond), where EChol and 5α-H,3α-ol show a small increase in T_m^{brd} and thus a reduced ability to

stabilize the gel state compared to Chol. While 5β-H,3α-ol has only a slightly negative T_m^{brd} curve when compared to T_m^{brd} for 5β-H,3β-ol (Fig 11D), the broadening of the phase transition follows the same pattern as that seen in the 3β-ols (5α-H, 5α-H, C5,6 double bond) even though $\Delta T_{\frac{1}{2}}^{brd}$ only increases to ~18 °C in 50 mol% EChol (Fig 11E). Although similar decreasing trends occur in the ΔH_m^{brd} of the 3α-ols compared to the 3β-ols (5α-H, 5α-H, C5,6 double bond), there are significant differences in that 5β-H,3α-ol reaches a peak maximum ΔH_m^{brd} value of about ~6 kcal/mol at 15 mol% and levels off to only ~5.5 kcal/mol by 50 mol%. Up to 30 mol% sterol, the ΔH_m^{brd} curve for 5α-H,3α-ol lies below that of EChol before switching positions. Both of these sterols are less able to abolish the phase transition relative to their 3β-ol counterparts, but the difference is less than that observed for the corresponding ΔH_m^{brd} values of the 5α-H sterols (3α-ol, 3α-ol) (Fig 11F). The steroids (5α-H, 5α-H, C5,6 double bond) behave very similarly to their 3α-ol counterparts in terms of their ability to cooperate and their ability to abolish the phase transition (Fig 12E and F, respectively), although the $\Delta T_{\frac{1}{2}}^{brd}$ curves either plateau or decrease slightly by ~2-3 °C at 50 mol% for all steroids. There are also differences in the T_m^{brd} curves for the steroids (5α-H, 5α-H, C5,6 double bond). The 5α-H steroid shows the smallest change in T_m^{brd} (Fig 12D) and thus gel-state stabilization, being essentially constant at all sterol concentrations. In contrast, CholK shows a decrease of ~1 °C by 15 mol%, holding steady at around 40 °C to 30 mol% steroid followed by a linear decrease of an additional 4 °C by 50 mol% steroid indicating a decrease in gel-state destabilization. 5β-H,3-K destabilizes the gel-state bilayer the most overall. However, the curve is concave above 25 mol% (Fig 12D), consistent with the appearance of additional endotherms in the heating thermograms below and above the main transition centered at ~22 °C and 52-58 °C, respectively (Fig 16). In a similar fashion, panel D of Figs 13-15 shows that the steroids more effectively destabilize the P_b' phase, whereas the 3β-ols are the least effective, with the exceptions of 5α-H,3α-ol being more
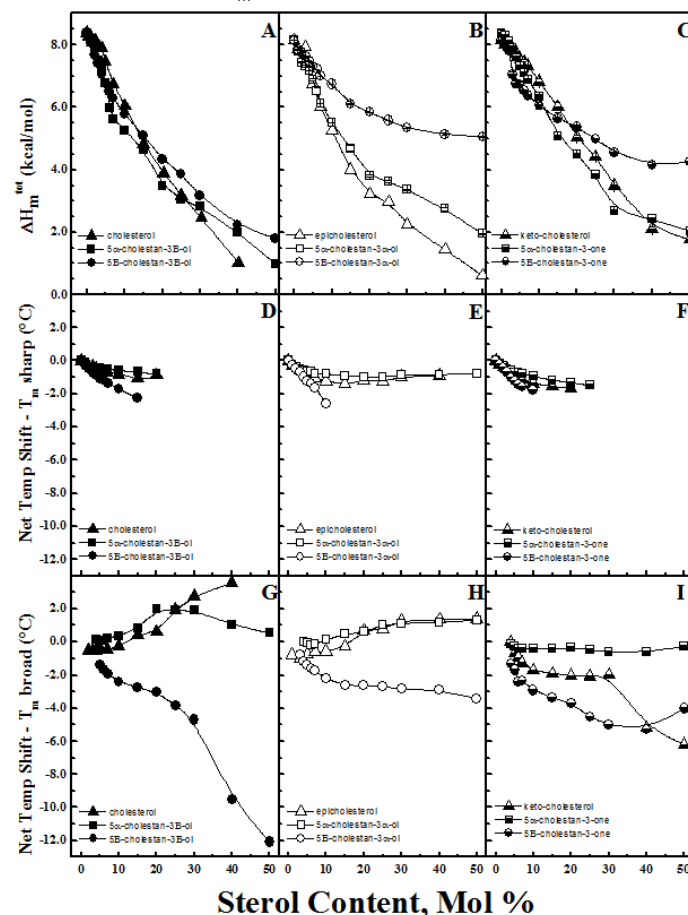
stabilizing above 40 mol% than 5α-H,3β-ol (Fig 14D) and 5β-H,3β-ol, which was the most effective at destabilizing the DPPC gel state at high sterol concentrations (Fig 15D).

*The effects of sterols on the total enthalpy component and net temperature shifts of the DPPC main phase transition*

Fig 17 (A-C) plots the ΔH_m^{tot} of all the sterol/DPPC systems. At less than 10 mol% sterol, Chol is the least effective of the 3β-ols in reducing ΔH_m^{tot}. At all sterol concentrations 5α-H,3β-ol more effectively reduces ΔH_m^{tot} than 5β-H,3β-ol, although above 30 mol%, Chol is the most effective 3β-ol (Fig 17A). The trends are more straightforward for the 3α-ols, with 5β-H,3α-ol being the least effective sterol in reducing ΔH_m^{tot} followed by 5α-H,3α-ol and EChol (Fig 17B). The behaviour is different again for the steroids, with 5β-H,3-K being the least effective in reducing the enthalpy at higher sterol concentrations, just like the 5β-H sterols (3α-ol, 3α-ol). However, below 10 mol%, 5β-H,3-K is best able to reduce ΔH_m^{tot}, intersecting with the curves of the other two steroids at ~10-20 mol%. From 15-40 mol%, 5α-H,3-K most effectively reduces ΔH_m^{tot}, whereas above 40 mol%, CholK is the most effective, as was evident with Chol and EChol (Fig 17C). This suggests that the C5,6 double bond plays an important role in favorable lipid/sterol interactions while reducing ΔH_m at high sterol concentrations. When

Figure 17. Total overall enthalpy (A, B, C; ΔHm) and net temperature shifts for the sharp (D,E, F; °C) and broad (G, H, I; °C) components of the sterol/DPPC binary mixtures studied, grouped by C-3 functional group. The left column is C-3β-hydroxyl sterols, the middle column is C-3α-hydroxyl sterols, and the right column is C-3-keto-sterols. When a standard error bar is not visible, it is less than or equal to the symbol dimensions. Data for cholesterol and epicholesterol is taken from Ref 24.

Mol %	Tm$_1$	$\Delta T_{1/2\ (1)}$	Tm$_2$	$\Delta T_{1/2\ (2)}$
20	22.09	0.81	52.67	2.36
25	21.92	1.10	53.14	1.94
30	21.85	1.19	53.28	2.72
40	21.87	0.91	58.55	1.13
50	22.07	0.80	58.63	0.80

Figure 16. Mass normalized DSC thermograms for 5β-cholestan-3-one/DPPC mixtures heated and cooled at 10 °C/h (to maximize resolution and minimize artifacts) illustrating sterol crystallite formation above and below and main chain-melting transition. The transition temperature and the half-widths of the endotherms are indicated on the graph.
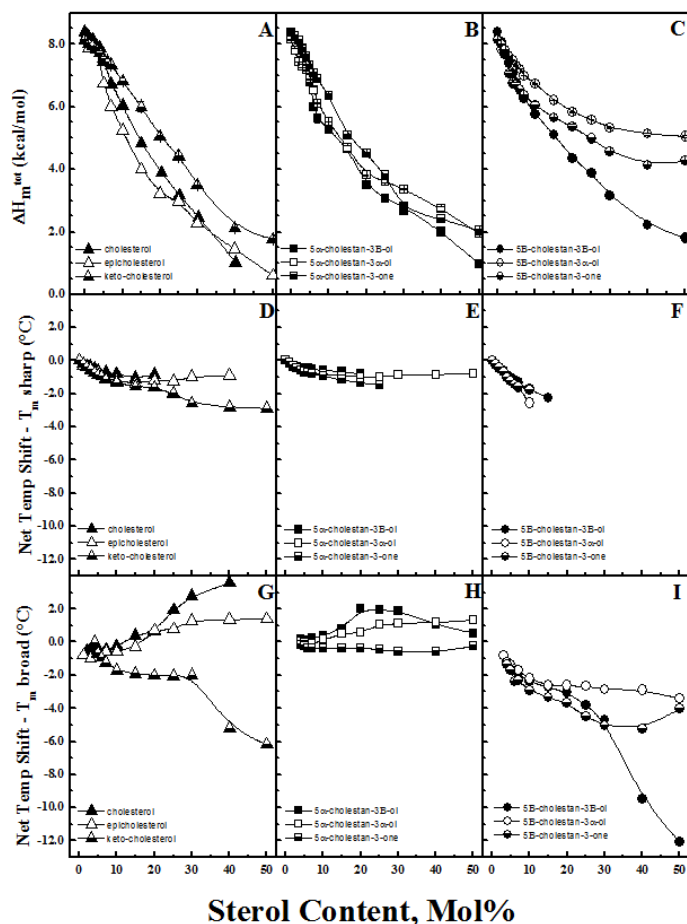
Figure 18. Total overall enthalpy (A, B, C; ΔHm) and net temperature shifts for the sharp (D, E, F; °C) and broad (G, H, I; °C) components of the sterol/DPPC binary mixtures grouped by C-5 conformation. The left column is C-5,6 double-bond sterols, the middle column is 5α-H sterols, and the right column is 5β-H sterols. When a standard error bar is not visible, it is less than or equal to the symbol dimensions. Data for cholesterol and epicholesterol is taken from Ref 24.

grouped by C5-conformation, CholK reduces ΔH_m^{tot} the least, and EChol is better than Chol to reduce enthalpy until about 40 mol% (Fig 18A). For the 5α-H and 5β-H groups, the 3β-ols are the most effective at reducing ΔH_m^{tot} at all sterol concentrations, whereas above 30 mol% the 3α-ols are less effective than the steroids. Below 30 mol% for the 5α-H group, the steroid was the least effective at ΔH_m^{tot} reduction, while 5β-H,3α-ol was the least effective of all the sterols and studies to reduce ΔH_m^{tot} at all concentrations (Fig 18B,C). An interpretation of this observation will follow in the Discussion.

A plot of the net temperature shift for both the sharp and broad components of all sterols are shown in Figs 17-18 D-F and G-I, respectively. The net temperature shift is defined as the temperature difference between the T_m of pure DPPC and the T_m^{shp} or T_m^{brd} measured from the DSC endotherms. Grouped by C3 functionality, it is evident that the 5α-H sterols are more perturbing than their 5α-H and C5,6-double bond counterparts for both the sharp and board components (Fig 17 D-I). However, when grouped by C5 conformation, the curves overlap nearly perfectly within each set of sterols, with slopes of the curves for the sharp endotherms more flat for the 5α-H and 5,6-double bond groups than the 5β-H group (3α-ol, 3α-ol, 3-K) (Fig 18 D-F). For the broad component, the steroids are more perturbing

for the C5,6-double bond and 5α-H groups than the corresponding sterols (3α-ol, 3α-ol) at all concentrations, as well as up to 30 mol% for 5β-H,3-K when compared to 5β-H(3α-ol, 3α-ol). Above 30 mol%, the net temperature shift for the broad component of 5β-H,3β-ol drops significantly, making it the most perturbing sterol at high sterol concentrations (Fig 18 D-I). This suggests that this sterol has a particularly unique packing arrangement that extremely disorders the bilayer structure.

Discussion

Effects of sterols on DPPC model membranes: structure and thermodynamics

The incorporation of a sterol molecule into the lipid bilayer disrupts the optimum packing between phospholipid molecules for a given phase structure. This produces a new packing geometry which will vary depending on the sterol/lipid mole ratio, the preference for self-association between like- and unlike-pairs arising from the directionality of associated local interactions, and the ability of water to enter into the bilayer interface. The relative rigidity of the sterol ring structure reduces the number of *cis-trans* isomerizations and kink formation in the neighbouring phospholipid acyl chains and has a differential disordering and ordering effect in the gel and L_a phase bilayers, respectively (26). Thus, changes in sterol configuration and conformation, including small changes in the OH rotamer population, may alter the balance between attractive and repulsive interactions within the lipid bilayer matrix. Each sterol chemical configuration will have different contributions to bilayer thermodynamic and structural factors that are dependent on phase state (30, 31). Unfortunately, relatively little is known about the independent contributions of the sterol ring system and alkyl side chains. This project has attempted to do some analysis on the ring system.

"Ideal" (C5α-H) versus "Native" (C5,6 Double Bond) Ring Conformations

The side-views of the 3D models of the C5,6 double bond and 5α-H sterol ring systems shown in Figs 2 and 3 illustrate that there is a slight difference in the energy minimized structures between the two sterol rings systems, with the double bond in the C5,6 system introducing a slight torsion at the ring A/B junction relative to the ideal, energy-minimum all-*trans* ring system of the C5α-H group with its 1,4 chair (cyclohexane) and envelope (cyclopentane) conformations. This structural change has mixed effects on the pretransition thermodynamic parameters. Chol and EChol are better at stabilizing the pretransition than their 5α-H counterparts, whereas 5α-H, K is more effective than CholK. Similarly, the C5,6 double bond group (3α-ol, 3α-ol, 3-K) is better at broadening the pretransition than the C5α-H group (3α-ol, 3α-ol, 3-K). In contrast, the C5α-H group (3α-ol, 3α-ol, 3-K) is better at abolishing the pretransition with the exception of CholK, which is more effective than 5α-H,3-K. See Table 1 for a summary of these trends.

The trends in the thermodynamic parameters are more consistent for the sharp and broad components of the main transition, and show that the 5α-H group (3α-ol, 3α-

ol, 3-K) more effectively stabilizes the main transition sharp component at all concentrations and also stabilizes the broad component below 40 mol%. The 5α-H group (3α-ol, 3α-ol, 3-K) also broadens and abolishes both main phase transition endotherms than the C5,6 group (3α-ol, 3α-ol, 3-K) at sterol concentrations below ~25-30 mol%, above which the trend reverses, and 5α-H,3β-ol, the closest structural analog to Chol, does not completely abolish the main transition at 50 mol% sterol as does Chol. These findings suggest that the double bond in Chol increases sterol miscibility with the DPPC bilayer at high sterol concentrations, similar to those found in erythrocyte and ocular lens membranes which contain up to 50 mol% and 70 mol% Chol, respectively (32).

"Distorted" (C5β-H) versus "Native" (C5,6 Double Bond) Ring Conformations

The side views of the 3D-models of the 5α-H sterols (Fig 4) illustrate that the 5α-H conformation significantly deviates from the *trans*-planar steroid nucleus found in the native C5,6 double bond (3α-ol, 3α-ol, 3-K) and in the optimum 5α-H groups (3α-ol, 3α-ol, 3-K). The trends in the thermodynamic parameters are more clear between the C5,6 double bond/5α-H groups (3α-ol, 3α-ol, 3-K) compared to the C5,6 double bond/5α-H groups (3α-ol, 3α-ol, 3-K). The C5,6 double bond group (3α-ol, 3α-ol, 3-K) is better able to stabilize the Lα phase, while the C5α-H group (3α-ol, 3α-ol, 3-K) is better able to broaden and abolish the transition. An exception arises for 5α-H,3-K, which demonstrates the worst ability to abolish the transition of all the ketones. The significance of this observation will be discussed later, including the similarities in the cooperativity of the pretransition behaviour for the 5α-H sterols and the steroids. See Table 1 for a summary of these trends.

For both the sharp and broad components of the main phase transition, we see that the 5α-H sterols (3α-ol, 3α-ol, 3-K) are the least able to stabilize the Pα phase, although they are better able to broaden and abolish the phase transition of the sterol-poor domain. For the broad component at almost all sterol concentrations, the C5,6 double bond group (3α-ol, 3α-ol, 3-K) more effectively broadens and abolishes the phase transition of the sterol-rich domain than the C5α-H group (3α-ol, 3α-ol, 3-K). This observed behaviour for the sterol-poor and sterol-rich domains suggests that the kink introduced at the A/B ring junction by the 5α-H limits the number of favorable interactions between the sterols and lipids. The kink effectively increases the molecular cross-sectional area, which significantly destabilizes the sterol-poor bilayer regions. The overall increase in cross-sectional area can be compensated by a change in the molecular tilt of the DPPC molecule, but it would also reduce the number of molecular

By C3 Functional Group										
		3β-OH			3α-OH			3-Ketone		
		Best	**Middle**	**Least**	**Best**	**Middle**	**Least**	**Best**	**Middle**	**Least**
Pretransition Ability to Stabilize/ Ability to Broaden/ Ability to Abolish	T_p	Chol	5α-H,3β-ol	5β-H,3α-ol	EChol	5α-H,3β-ol	5β-H,3α-ol	5α-H,3-K	CholK	5β-H,3-K
	$\Delta_{T½p}$	5β-H,3β-ol (<4 mol%) Chol (>4mol%)	5α-H,3β-ol	Chol (<2 mol%) 5β-H,3β-ol (>4mol%)	EChol	5β-H,3α-ol	5α-H,3α-ol	5β-H,3-K	CholK	5α-H,3-K
	ΔH_p	5β-H,3β-ol	5α-H,3β-ol	Chol	5α-H,3α-ol	5β-H,3α-ol	EChol	CholK	5β-H,3-K (>4 mol%) 5α-H,3-K (<4 mol%)	5α-H,3-K (<4 mol%) 5β-H,3-K (>4 mol%)
Sharp Component Ability to Stabilize/ Ability to Broaden/ Ability to Abolish	T_m^{shp}	5α-H,3β-ol	Chol	5β-H,3β-ol	5α-H,3α-ol	EChol	5β-H,3α-ol	5α-H,3-K	CholK	5β-H,3-K
	$\Delta T_½^{shp}$	5β-H,3β-ol	5α-H,3β-ol	Chol	5β-H,3α-ol	EChol	5α-H,3α-ol	5β-H,3-K (<7mol%) CholK (>7mol%)	CholK (<7mol%) 5β-H,3-K (>7mol%)	5α-H,3-K
	ΔH_m^{shp}	5α-H,3β-ol (<7 mol%) Chol (>7 mol%)	Chol (<7 mol%) 5α-H,3β-ol (>7 mol%)	5β-H,3β-ol	5β-H,3α-ol	EChol	5α-H,3α-ol	5β-H,3-K	5α-H,3-K (<15 mol%) CholK (>15 mol%)	CholK (<15 mol%) 5α-H,3-K (>15 mol%)
Broad Component Ability to Stabilize/ Ability to Broaden/ Ability to Abolish	T_m^{brd}	5α-H,3β-ol (<25 mol%) Chol (>25 mol%)	Chol (<25 mol%) 5α-H,3β-ol (>25 mol%)	5β-H,3β-ol	5α-H,3α-ol (<25 mol%) Chol (>25 mol%)	Chol (<25 mol%) 5α-H,3α-ol (>25 mol%)	5β-H,3α-ol	5α-H,3-K	CholK (< 40 mol%) 5β-H,3-K (>40 mol%)	5β-H,3-K (<40 mol%) CholK (>40 mol%)
	$\Delta T_½^{brd}$	5β-H,3β-ol (<25 mol%) Chol (>25 mol%)	Chol (<25 mol%) 5α-H,3β-ol (>25 mol%)	5α-H,3β-ol (<25 mol%) 5β-H,3β-ol (>25 mol%)	EChol	5β-H,3α-ol	5α-H,3α-ol	CholK	5β-H,3-K (<30 mol%) 5α-H,3-K (>30 mol%)	5α-H,3-K (<30 mol%) 5β-H,3-K (>30 mol%)
	ΔH_m^{brd}	Chol	5α-H,3β-ol	5β-H,3β-ol	5α-H,3α-ol (<30 mol%) EChol (>30 mol %)	EChol (<30 mol%) 5α-H,3α-ol (>30 mol %)	5β-H,3α-ol	5α-H,3-K (<40 mol%) CholK (>40 mol%)	CholK (<40 mol%) 5α-H,3-K (>40 mol%)	5β-H,3-K
Total Enthalpy Ability to Abolish	ΔH_m^{tot}	5α-H,3β-ol (<30 mol%) Chol (>30 mol%)	Chol (<30 mol%) 5α-H-3β-ol (>30 mol%)	5β-H,3β-ol	EChol	5α-H,3α-ol	5β-H,3α-ol	CholK (<10 mol%) 5α-H,3-K (>10 mol%, <40 mol%) CholK (>40 mol%)	CholK (>15 mol%, <40 mol%) 5α-H,3-K (>40 mol%)	5β-H,3-K (>15 mol%)

Table 1. Observation summaries for the pretransition (Pretransition row) and main phase transition (Sharp Component, Broad Component, and Total Enthalpy rows) arranged by C3 functional group (3β-ol, 3α-ol, 3-K). T (°C) ranks the ability of the sterols to stabilize either the Lβ' (pretransition) or Pβ' (main phase transition) phases, ΔT½ (°C) ranks the ability of the sterols to broaden the respective transition, and ΔH (kcal/mol) ranks the ability of the sterols to abolish the respective transition.

contacts within the hydrocarbon chain region. As a consequence, the overall number of favorable interactions with the lipid bilayer would decrease more rapidly for DPPC mixtures containing a kinked sterol than for sterols with smaller cross-sectional areas like the C5α-H group (3α-ol, 3α-ol, 3-K). This may explain why the C5α-H group (3α-ol, 3α-ol, 3-K) much more rapidly reaches its miscibility limit in the sterol-rich DPPC domain.

3α-ols versus 3β-ols

A comparison of the DSC measurements obtained for the pretransition of DPPC mixtures containing low concentrations of either 3α-ols or 3α-ols whose hydroxyl group orientations are equatorial and axial, respectively, found that the 3α-ols more effectively stabilize the Lα' phase and broaden the pretransition more effectively than the corresponding 3α-ols. See Table 2 for a summary of these trends. The same relationship exists between OH-group orientation and the ability of the sterol to abolish the pretransition, with the exception of the 5α-H group, where the 3α-ol is more effective than the 3α-ol. In the case of the sharp component of the main transition, 3α-ols more effectively stabilize the Pα' phase and broaden the sterol-poor domain phase transition than the 3α-ols. However, the sharp component persists up to 40 and 50 mol% in both EChol and 5α-H,3α-ol, respectively, and suggests that there is a change in the balance of sterol- poor and sterol-rich stoichiometries in favor of the former. Within the main phase transition broad component of the 3α/α-ols, Chol (3α-ol) better stabilizes the gel phase than EChol (3α-ol), 5α-H,3α-ol (3α-ol) better stabilizes the gel phase than 5α-H,3α-ol (3α-ol) at >40 mol% sterol concentrations and 5α-H,3α-ol (3α-ol) better stabilizes the gel phase than

5α-H,3α-ol (3α-ol) at all sterol concentrations. However, in all cases, the 3α-ols always more effectively broaden and abolish the broad endotherms than the 3α-ols and more so at high sterol concentrations. Previous work with EChol suggested that the sterol sits lower in the bilayer interface, which would result in decreased hydrogen-bonding interactions at the lipid-water interface (24). It appears that we are looking at two perturbing mechanisms here, one related to cross-sectional area and the other to the sterol depth in the bilayer. DSC alone, however, is unable to distinguish the extent to which either of these mechanisms perturbs bilayer structure.

Steroids versus Sterols

There are few consistent relationships between the steroids and the sterols other than the steroids (5α-H, 5α-H, C5,6 double bond) show significant inabilities to stabilize, broaden and abolish both the pretransition and main-chain melting transitions relative to the sterols. However, especially notable are the significant differences in $\Delta T_{p\frac{1}{2}}$ in the steroids (5α-H, 5α-H, C5,6 double bond) (and also 5α-H,3α-ol and 5α-H,3α-ol) with increasing sterol concentration, suggesting the presence of multiple endothermic peaks in the pretransition of these sterol/DPPC mixtures. As suggested earlier, the major contributor to this behaviour for the 5α-H group may arise from the kink in the A-B ring junction, which increases the cross-sectional area of the steroid nucleus and preventing molecular packing and favourable interactions with neighbouring DPPC molecules. This could increase the number of chemical environments seen by the sterol molecule. A similar behaviour may occur upon oxidizing the C3-OH functional group to a ketone, where the polarizability of

By C5 Conformation										
		5,6-double bond			**5α-H**			**5β-H**		
		Best	**Middle**	**Least**	**Best**	**Middle**	**Least**	**Best**	**Middle**	**Least**
Pretransition Ability to Stabilize/ Ability to Broaden/ Ability to Abolish	T_p	EChol	Chol	CholK	5α-H,3-K	5α-H,3α-ol	5α-H,3β-ol	5β-H,3α-ol	5β-H,3β-ol	5β-H,3-K
	$\Delta T_{\frac{1}{2}p}$	EChol	Chol	CholK	5α-H,3β-ol	5α-H,3α-ol	5α-H,3-K	5β-H,3α-ol	5β-H,3-K	5β-H,3β-ol
	ΔH_p	CholK	EChol	Chol	5α-H,3α-ol	5α-H,3β-ol (<4 mol%) 5α-H,3-K (>4 mol%)	5α-H,3-K (<4 mol%) 5α-H,3β-ol (>4 mol%)	5β-H,3β-ol	5β-H,3-K	5β-H,3α-ol
Sharp Component Ability to Stabilize/ Ability to Broaden/ Ability to Abolish	T_m^{shp}	Chol	EChol	CholK	5α-H,3β-ol	5α-H,3α-ol	5α-H,3-K	5β-H,3β-ol	5β-H,3-K	5β-H,3α-ol
	$\Delta T_{\frac{1}{2}}^{shp}$	CholK	EChol (<15 mol%) Chol (>15 mol%)	Chol (<15 mol%) Echol (>15 mol%)	5α-H,3β-ol	5α-H,3-K	5α-H,3α-ol	5β-H,3-K (<10 mol%) 5β-H,3β-ol (>10 mol%)	5β-H,3β-ol (<10 mol%) 5β-H,3-K (>10 mol%)	5β-H,3α-ol
	ΔH_m^{shp}	EChol (<20 mol%)	Chol	CholK	5α-H,3β-ol	5α-H,3-K	5α-H,3α-ol	5β-H,3-K = 5β-H,3α-ol	5β-H,3-K = 5β-H,3α-ol	5β-H,3β-ol
Broad Component Ability to Stabilize/ Ability to Broaden/ Ability to Abolish	T_m^{brd}	Chol	EChol	CholK	5α-H,3β-ol (<40 mol%) 5α-H,3α-ol (>40 mol%)	5α-H,3α-ol (<40 mol%) 5α-H,3β-ol (>40 mol%)	5α-H,3-K	5β-H,3α-ol	5β-H,3β-ol (<30 mol%) 5β-H,3-K (>30 mol%)	5β-H,3β-ol (<30 mol%) 5β-H,3-K (>30 mol%)
	$\Delta T_{\frac{1}{2}}^{brd}$	Chol	EChol	CholK	5α-H,3β-ol	5α-H,3-K	5α-H,3α-ol	5β-H,3β-ol	5β-H,3-K	5β-H,3α-ol
	ΔH_m^{brd}	EChol (<40 mol%) Chol (>40 mol%)	Chol (<40 mol%) EChol (>40 mol%)	CholK	5α-H,3α-ol <40 mol% 5α-H,3β-ol (>40 mol%)	5α-H,3β-ol (<40 mol%) 5α-H,3α-ol (>40 mol%)	5α-H,3-K	5β-H,3β-ol	5β-H,3-K	5β-H,3α-ol

Table 2. Observation summaries for the pretransition (Pretransition row) and main phase transition (Sharp Component, Broad Component, and Total Enthalpy rows) arranged by C5 conformation (5,6 double-bond, 5α-H, 5β-H). T (°C) ranks the ability of the sterols to stabilize either the Lβ' (pretransition) or Pβ' (main phase transition) phases, ΔT½ (°C) ranks the ability of the sterols to broaden the respective transition, and ΔH (kcal/mol) ranks the ability of the sterols to abolish the respective transition.

the nuclear polar group is reduced and the ability of the steroid to act as a hydrogen bond donor to the carbonyl of the acyl chains in the DPPC bilayers is eliminated, meaning that hydrogen bonding is only possible with water. One possible explanation for this behaviour is that the rippled gel phase exists in two isomorphs differing in periodicity and that the steroids (5α-H, 5α-H, C5,6 double bond) and the 5α-H sterols (3α-ol, 3α-ol) shifts the balance between these two related phase structures (33).

Reduced polarizability and an inability to donate hydrogen bonds would suggest that the steroids sit much lower in the bilayer. This idea has been confirmed by molecular model simulations (34, 35), and these same simulations illustrate that substituting the hydroxyl group with a ketone promotes the translocation or flip-flopping of steroids between the leaflets. Further, 3-ketone functional groups are usually found in nature in steroid hormones like testosterone and estrogen that usually must diffuse or be transported through cellular bilayers to reach their target, like the cellular nucleus where they activate transcription factors. This suggests then that the ketone group prevents steroids from having a prolonged residence in either membrane leaflet. Hence, the combination of the 5α-H conformation and a ketone functional group would create a steroid with extreme miscibility problems (discussed in next section).

The deeper penetration of sterols has been postulated to increase the ordering and condensation of PC bilayers (36, 37). This has been supported by Chol/EChol studies using both FTIR (Chol/EChol) and molecular simulations (24, 38), which implies that further information as to where these sterols are sitting in the bilayer may come to light though Fourier transform infrared spectroscopy studies. While DSC can provide valuable thermodynamic data about the phase state and organization of lipid assemblies and how these structure and physical properties are modulated by membrane constituents, it is not a structural technique. Hence, DSC is most valuable at interpretation sterol/lipid interactions when it is combined with a direct structural technique such as FTIR, NMR, or X-ray diffraction (39).

Sterol Immiscibility and Optimal Lipid-Sterol Stoichiometries

At the boundary between sterol-poor and sterol-rich domains, the further addition of sterol into the DPPC bilayer does not result in a homogenous sterol distribution in the bilayer but the creation of different lipid/sterol microdomains (40). These domains exist in both gel and liquid-crystalline phase regions and may differ in both their physical properties and composition up to a critical miscibility point. Hence, similar slopes below $\Delta H_m^{brd-max}$ within a subset (Figs 10-15 F) suggest similar sterol/DPPC stoichiometries or domain structures for the parent chemical configuration (for example, 5α-H, 5α-H, C5,6 double bond), whereas significant differences in slope probably reflect a change in the balance between the various lipid/sterol domains or a change in domain structure.

$\Delta H_m^{brd-max}$ represents a critical miscibility point where at least two domains containing different sterol-lipid populations coalesce. At higher sterol concentrations, the

sterol/lipid dispersion is uniform and increasing amounts of sterol partition uniformly into the bilayer, effectively increasing the sterol/lipid ratio. However, full miscibility can only occur if the balance between like/like and like/unlike pairs favours the latter. When the like/unlike interactions are strong and the molecular packing is ideal, $\Delta H_m^{brd} = 0$, as is seen for Chol. This means that if $\Delta H_m^{brd} \neq 0$ for specific sterol/DPPC mixtures, then either the balance between like/like and like/unlike pairs is not ideal, or there are fewer or weaker favorable interactions between like/unlike pairs. Therefore, full miscibility is not achieved and may not be possible. Also, differences in the magnitude of $\Delta H_m^{brd-max}$ among different sterol chemical structures probably arise from the different ability of each sterol to disrupt the lipid/sterol interactions of the dominant domain. A possible reason for this may include the formation of a highly-ordered molecular packing with very strong like/unlike interactions. Thus, by virtue of differences in the strength and number of like/unlike interactions, each sterol structure will determine the number of different lipid domains, their composition, and, potentially, their physical structure. The formation of each domain structure will occur at a critical point away from or close to the phase transition of the mixture (41-43). The stability of each domain is determined by the ease with which additional sterol molecules can be incorporated into that specific domain structure. "Stable" domains have a greater sterol insertion energy which will vary with sterol structure and will also be concentration dependent. This would explain the variation in $\Delta H_m^{brd-max}$ in both the concentration and enthalpy context.

An example of immiscibility in these DPPC mixtures where the balance between like/like and unlike/like interactions is not altered is the 5α-H sterol conformation where the kink at the ring A/B junctions increases the overall steric bulk of the molecule. The effect of the change in the ring A orientation cannot explain the significantly greater $\Delta H_m^{brd-max}$ and the inability of 5α-H,3α-ol to abolish the phase transition relative to that of 5α-H,3α-ol. Therefore, the observations for the 5α-H sterols (3α-ol, 3α-ol) suggest that if the earlier interpretation of the $\Delta H_m^{brd-max}$ is valid, the combination of the 3α-OH and 5β-H, 10b-CH$_3$ (*cis*) configurations produces a sterol molecule that has fewer favorable interactions in the interfacial and hydrocarbon chair regions with neighboring DPPC molecules and, therefore, cannot form stable domains in the DPPC bilayer. This sterol would be unable to maintain a high sterol/PC concentration in the bilayer and would not be fully miscible with DPPC. In the corresponding 5β-H,3β-ol, partial miscibility is restored by stronger intermolecular interactions with DPPC in the bilayer interface with the change in C3-hydroxyl orientation.

The inability of all the sterols and steroids studied here other than Chol to abolish the main phase transition at high sterol concentrations has been noted with other sterols (23-25) and comes as no surprise if Chol is assumed to have to have the ideal structure for packing and optimal miscibility in DPPC bilayers. The location of the immiscible sterol pool is not clear when DSC in unable to detect those separate phases like those found in the 5β-H,3-K/DPPC mixtures, where phase transitions arising from

phase separated crystalline sterols is observed at higher steroid concentrations (Fig 16). The significant increase in the area of the crystallite endotherm above the phase transition is accompanied by the sudden increase in T_m^{brd} and decrease in $\Delta T_{1/2}^{brd}$ at 50 mol% concentration for 5β-H,3-K (Fig 12 D,E). Nucleation of crystalline 5α-H,3-K occurs in the bilayer and then the sterol partitions out into the bulk phase changing the thermodynamic parameters of the 50% mol 5α-H,3-K/DPPC mixture to one more closely resembling a sample containing 25-30 mol% steroid. To a lesser degree, these same changes in T_m^{brd} and $\Delta T_{1/2}^{brd}$ are seen for 5α-H,3-K, although no crystallites are visible in thermograms obtained from mixtures containing higher sterol concentrations. Their absence may be due to a lack of instrument sensitivity and the poorly-energetic nature of these weak transitions. This is plausible given that the total enthalpy curves for both the 5α-H and 5α-H steroids level off rapidly above 30 mol% concentration. Interestingly, the total enthalpy curve does not level off as readily for CholK and is the most able of the steroids to abolish the DPPC main transition. CholK also shows a significant ability to perturb the DPPC bilayers at these sterol concentrations, lending additional support to the conclusion made earlier that the C5,6 double bond provides additional stabilizing interactions with DPPC in the bilayer at physiologically-relevant sterol concentrations.

Concluding Remarks

The Venn diagram presented in Fig 19 summarizes the ability of the various sterols and steroids studied to stabilize the Pα' phase and broaden and abolish the DPPC Pα'/Lα phase transition. Chol is best able to stabilize the Pα' phase and broaden and abolish the DPPC main phase transition. Moving outwards, the other C5,6 double bond (EChol, CholK) and C5α-H group members (3α-ol, 3α-ol, 3-K) show abilities to meet at least two of these criteria. The 5α-H group (3α-ol, 3α-ol, 3-K) shows significantly diminished capabilities, with 5α-H,3-K being distinct from other members of the global set. In a general sense, we see that an all-*trans* ring system is required to stabilize the Pα' phase, a 3α-OH functional group to broaden the transition, and the presence of the C5,6-double bond to abolish the transition. Hence, changes in the chemical structure of the sterol nucleus influence the bilayer thermodynamic properties, such as the gel/L_a phase transition temperature and cooperativity, the ability to abolish the chain-melting phase transition and the miscibility of the sterol in the lipid bilayer. The changes in sterol chemical structure are also known to affect the molecular tilt (44), the headgroup/hydrocarbon chain packing geometry, hydration, curvature and, consequently, the membrane nonlamellar phase preference (45-47). Our observations lend support to the Bloch hypothesis, which suggested that there was a progressive change in the ability of the intermediates in Chol biosynthesis to pack into a phospholipid bilayer and that lanosterol (the earliest intermediate) is the poorest fit and Chol (the end product) is the best. This proposes that this energy-expensive conversion process, which produces a sterol with optimum molecular packing abilities in the phospholipid bilayer, has considerable evolutionary
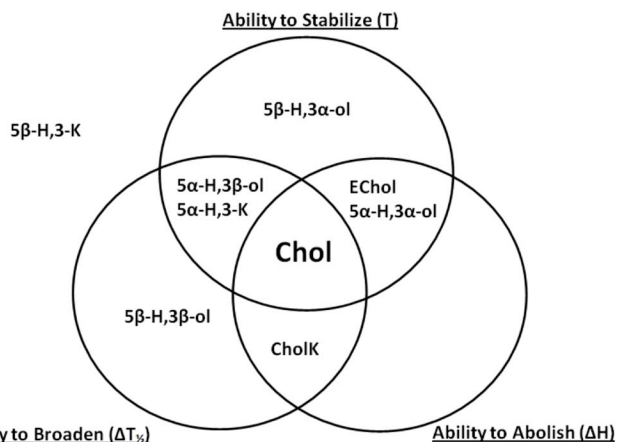
Figure 19. Venn diagram illustrating the ability of each sterol to stabilize the gel phase (T), and broaden (ΔT½) and abolish the main phase transition (ΔH) at high (biologically relevant) sterol concentrations.   Cholesterol meets all three parameters while 5β-H,3-K fails to reasonably satisfy any of the parameters relative to the other sterols studied. Overall, sterols with a C5,6 double bond and C5α-H conformation are best able to stabilize the Lβ' phase. The 3β-OH sterols are the best at broadening the main phase transition, while the sterols with the C5,6 double bond conformation are best able to abolish the main phase transition.

significance (48).

Given the differences in the thermodynamic parameters obtained from DPPC mixtures containing different sterol ring configurations and their associated changes in bilayer stability and miscibility, it becomes clear that changing the sterol chemical configuration has a significant effect on the bilayer physical properties. Thus, any sterol molecule whose ring structure deviates from that of Chol is unlikely to be fully miscible in the mammalian cell membrane, and an *in vivo* change in ring structure brought about by, for example, oxidation of 3α-OH by Chol oxidase followed by the removal of the SpM headgroup would destabilize the physical structure of the lipid rafts. Such an event, which has been reported in many human diseases (see the Introduction), would result in a signaling cascade leading to cell death and disease manifestation. Hence, understanding the variation in the strength, number, and type of interactions between the sterol ring system and neigbouring phospholipid molecules is an important part of understanding the disease process and prospective membrane-associated therapies.

References

1. Hartmann, T., Kuchenbecker, J., Grimm, M.O.W. (2007) J. Neurochem. 103: 159–170.

2. D'Errico, G., Vitiello, G., Ortona, O., Tedeschi, A., Ramunno, A., D'Ursi, A.M. (2008). Biochim. Biophys. Acta. 1778: 2710–2716.

3. Sacchetti, P., Sousa, K.M., Hall, A.C., Liste, I., Steffensen, K.R., Theofilopoulos, S., Parish, C.L., Hazenberg, C., Richter, L.A., Hovatta, O., Gustafsson, J.-A., Arenas, E. (2009) Cell Stem Cell 5: 409–419.

4. Chazal, N., Gerlier, D. (2003) Microbiol. Mol. Biol. Rev. 67: 226-37 .

5. Ablan, S., Rawat, S.S., Viard, M., Wang, J.M., Puri, A., Blumenthal, R.

(2006) Virol. J. 3: 104. PMID: 17187670.

6. Waheed, A.A., Freed, E.O., (2009) Virus Res. 143: 162-176.

7. Wadia, J.S., Schaller, M., Williamson, R.A., Dowdy, S.F. (2008) PLoS ONE 3: e3314. doi:10.1371 /journal.pone.0003314.

8. Zhong, J., Yang, C., Zheng, W., Huang, L., Hong, Y., Wang, L., Sha, Y. (2009) Biophys. J. 96: 4610-21. Erratum in: Biophys J. 97: 397.

9. van der Meer-Janssen, Y.P.M., van Galen, J., Batenburg, J.J., Helms, J.B. (2010) Prog. Lipid Res. 49: 1-26.

10. Panda, S., Jafri, M., Kar, A., Meheta, B.K. (2009) Fitoterapia 80: 123-126.

11. Woyengo, T.A., Ramprasath, V.R., Jones, P.J.H. (2009) Eur. J. Clin. Nutr. 63: 813–820.

12. Carpinteiro, A., Dumitru, C., Schenck, M., Gulbins, E. (2008) Cancer Lett. 264: 1-10.

13. Barenholz, Y. (2004) Subcell. Biochem. 37: 167-215.

14. Cremesti, A.E., Goni, F.M., Kolesnick, R. (2002) FEBS Lett. 531: 47-53.

15. Biasi, F., Mascia, C., Astegiano, M., Chiarpotto, E., Nano, M., Vizio, B., Leonarduzzi, G., Poli, G. (2009) Free Rad. Biol. Med. 47: 1731-1741.

16. Ramstedt, B., Slotte, J.P. (2006) Biochim. Biophys. Acta 1758: 1945-56.

17. Goñi, F.M., Alonso, A. (2009) Biochim. Biophys. Acta. 1788: 169-77.

18. Maggio, B., Borioli, G.A., Del Boca, M., De Tullio, L., Fanani, M.L., Oliveira, R.G., Rosetti, C.M., Wilke, N. (2008) Cell Biochem. Biophys. 50: 79-109.

19. Mannock, D.A., McIntosh, T.J., Jiang, X., Covey, D.F., McElhaney, R.N. (2003) Biophys. J. 84: 1038-1046.

20. McMullen, T.P.W., Lewis, R.N.A.H., McElhaney. R.N. (1993) Biochemistry. 32: 516-522.

21. McMullen, T.P.W., Lewis, R.N.A.H., McElhaney. R.N. (1994) Biophys. J. 66: 741-752.

22. McMullen, T.P., Lewis, R.N.A.H., McElhaney, R.N. (2009) Biochim. Biophys. Acta 1788: 345-57.

23. Mannock, D.A., Lewis, R.N.A.H., McElhaney, R.N. (2006) Biophys. J. 91: 3327–3340.

24. Mannock, D.A., Lee, M.Y., Lewis, R.N.A.H., McElhaney, R.N. (2008) Biochim. Biophys. Acta. 1778: 2191-202.

25. Mannock, D.A., Lewis, R.N.A.H., McElhaney, R.N. (2010) Biochim. Biophys. Acta. 1798: 376–388.

26. Mannock, D.A., Lewis, R.N.A.H., McMullen, T.P.W., McElhaney, R.N. (2010) CPL. doi:10.1016/j.chemphyslip.2010.03.011.

27. McNamara, D.J., Pria, A, Miettinen, T.A. (1981) J. Lipid Res. 22: 474-484.

28. Javiltt, N.B. (2002) BBRC. 292: 1147-1153.

29. Lewis, R.N.A.H., Mannock, D.A., McElhaney, R.N. (2007) Differential scanning calorimetry on the study of lipid phase transitions in model and biological membranes: practical considerations, in: A. Dopico (Ed.), Methods in Membrane Lipids, Humana Press, Totown, New Jersey, pp. 171–195.

30. Quindnero, D., Frontera, A., Escudero, D., Ballester, P., Costa, A., Deya, P.M. (2008) Theor. Chem. Account. 120: 385-293.

31. Estarellas, C., Frontera, A., Qunidenero, D., Alkorla, I, Deya, P.M. (2009) J. Phys. Chem. A. 113: 3266-3273.

32. Rog, T., Pasenkiewicz-Gierula, M, Vallulainen, I., Karttunen, M. (2009) Biochim. Biophys. Acta. 1788: 97-121.

33. Katsaras, J., Kucerka, N., Nieh, M. (2008) Biointerphases. 3: F55-F63.

34. Rog, T., Stimson, L.M., Paskenkewicz-Gierula, M., Vallulainen, I., and Karttunen, M. (2008) J. Phys. Chem. B. 112, 1946-1952.

35. Berring, E.E., Borrenphol, K., Fliesler, S.J., Serfis, A.R.. (2005) CPL. 136: 1-12.

36. Rog, T., and Paskenkewicz-Gierula, M. (2006) Biophys. J. 91, 3756-3767.

37. Rog, T., and Paskenkewicz-Gierula, M. B(2006) iochemie. 88, 449-460.

38. Rog, T., and Pasenkiewicz-Gierula, M. (2003) Biophys. J. 84, 1818-1826.

39. Lewis, R.N.A.H, Mannock, D.A., McElhaney, R.N. (2008) Differential Scanning Calorimetry to Study Lipids and Lipid Membranes, in Wiley Encyclopedia of Chemical Biology. John Wiley & Sons, Inc. doi: 10.1002/9780470048672.wecb049.

41. Veatch, S.L., Sunbias, O., Keller, S.L., Ganrisch, K. (2007). PNAS. 104: 17650-17655.

42. Veatch, S.L. (2007). SCDB. 16: 573-582.

43. Veatch, S.L., Keller, S.L., Biochim. Biophys. Acta. (2005). 1746: 172-285.

44. Cournia, Z, Ullmann, G.M., Smith, J.C. (2007) J Phys. Chem. B. 111: 1786-1801.

45. Wang X., Quinn, P.J. (2002). Biochim. Biophys. Acta 1564: 66-72.

46. Bacia, K., Schwille, P., Kurzchalia, T. (2005) Proc. Nat. Acad. Sci. USA. 102: 3272-3277.

47. Tenchov, B.G., MacDonald, R.C., Siegel, D.P. (2006) Biophys. J. 91: 2508-2518.

48. Bloch, K. (1983) CRC Crit. Rev. Biochem.